ARTICLES
https://doi.org/10.1038/s41561-019-0315-9
nature geoscience

Increased landslide activity on forested hillslopes following two recent volcanic eruptions in Chile

Oliver Korup[1,2*], Jan Seidemann[1] and Christian H. Mohr[1]

Large explosive eruptions can bury landscapes beneath thick layers of tephra. Rivers subsequently overloaded with excess pyroclastic sediments have some of the highest reported specific sediment yields. Much less is known about how hillslopes respond to tephra loads. Here, we report a pulsed and distinctly delayed increase in landslide activity following the eruptions of the Chaitén (2008) and Puyehue–Cordón Caulle (2011) volcanoes in southern Chile. Remote-sensing data reveal that landslides clustered in densely forested hillslopes mostly two to six years after being covered by tephra. This lagged instability is consistent with a gradual loss of shear strength of decaying tree roots in areas of high tephra loads. Surrounding areas with comparable topography, forest cover, rainfall and lithology maintained landslide rates roughly ten times lower. The landslides eroded the landscape by up to 4.8 mm on average within 30 km of both volcanoes, mobilizing up to 1.6 MtC at rates of about 265 tC km^{-2} yr^{-1}. We suggest that these yields may reinforce the elevated river loads of sediment and organic carbon in the decade after the eruptions. We recommend that studies of post-eruptive mass fluxes and hazards include lagged landslide responses of tephra-covered forested hillslopes, to avoid substantial underestimates.

Explosive volcanic eruptions disturb landscapes and ecosystems by mantling hillslopes with tephra loads that smother and poison vegetation, seal and sterilize soils, impact habitats, and alter infiltration rates and surface runoff[1,2]. Surface runoff and lahars reworking this tephra cover prompt some of the highest known sediment yields in rivers[3], catastrophically raising and shifting channel beds, and covering floodplains. How quickly landscapes and ecosystems recover from explosive eruptions depends not only on controls such as the mass, volume, chemistry and spatial distribution of tephra released, but also on subsequent feedbacks between biotic and abiotic processes that often remain conceptual and rarely quantified[4]. Ecologists have long recognized that pyroclastic fallout can be a major disturbance to forests[5,6], whereas geomorphologists have noted that damaged tree cover can enhance post-eruptive erosion[7] and river loads of particulate organic carbon[8]. Quantifying how forest dieback compromises slope stability—a lesson learnt from many non-volcanic settings[9–11]—is an open research question that we address here. To this end, we report a distinct episode of landslides on tephra-covered hillslopes surrounding two volcanoes that erupted between 2008 and 2012 in the Andean Southern Volcanic Zone (SVZ). We hypothesize that these landslides are causally linked to the eruptions, and aim to explain their causes and quantify their impact.

We focus on the Pleistocene to Holocene Chaitén (42.83° S 72.65° W) and Puyehue (40.59° S 72.12° W) volcanoes that straddle the active right-lateral, strike-slip Liquiñe–Ofqui Fault Zone[12] along the southern Chilean Andes, and receive several metres of annual precipitation[5]. In 2008, Chaitén Volcano gave rise to a rare sequence of explosive rhyolitic eruptions[13] entailing pyroclastic density currents, minor lateral blasts, lava-dome growth and collapse, and widespread tephra falls of an estimated 0.5–1.0 × 10^9 m^3 (ref. [14]). The 2011 eruption of a vent in the Puyehue–Cordón Caulle volcanic complex[12] produced a rhyolitic lava flow, several pyroclastic density currents and widespread fall of roughly 0.5–1.5 × 10^9 m^3 of tephra over the Andes and Patagonia[15]. Both eruptions impacted the Valdivian rainforests—a global biodiversity hotspot[16,17] featuring Chile's densest forest cover, and one of the world's largest continuous rainforest areas dominated by *Nothofagus* species, *Eucryphia cordifolia*, *Drimys winteri*, *Laureliopsis philippiana*, *Weinmannia trichosperma* and *Caldcluvia paniculata* with up to 850 t ha^{-1} of living biomass and up to twice as much soil organic carbon[8].

Post-eruptive landslides cluster in tephra-covered forests

Landsat images from 2000–2014[18] show widespread post-eruptive losses of these dense rainforests around Chaitén and Puyehue volcanoes, involving 151 and 321 km^2, respectively (Fig. 1), or 27% of all Patagonian forest losses south of 40° S during that period. The eruptions caused the largest natural loss of adjoining forest areas in Chile between 2000 and 2014—much larger than, for example, the forest areas eroded by landslides triggered by the 2007 magnitude 6.2 Aysén Fjord earthquakes[8]. The imagery reveals a distinct browning (a decrease in the normalized difference vegetation index (NDVI)) where thick pyroclastic deposits had covered the native vegetation. Forest losses were negligible before these eruptions, but peaked sharply and decayed thereafter. Average rates of landslide activity, expressed as the total area affected by slope failures per year, were an order of magnitude lower in the years before the eruptions (Fig. 2). Landslide activity increased markedly after the eruptions, and without any noticeable change in rainfall conditions (see Supplementary Information, Supplementary Figs 1–3 and Supplementary Tables 1 and 2). Between April 2012 and November 2016, at least 617 debris slides and debris flows eroded >10.8 km^2 of densely forested hillslopes within 30 km of Chaitén Volcano (Supplementary Figs. 4 and 5 and Supplementary Tables 3 and 4). At Puyehue, at least 133 landslides eroded >2.5 km^2 between April 2012 and November 2016 within a 23 km radius from the vent (Fig. 3), affecting more area there than the landslides triggered by the 1960 Valdivia earthquake[17], which had a magnitude of ~9.5. Forest losses were lower at Puyehue because this volcano is higher (~2,200 m above sea level) than Chaitén (~1,100 m above sea level), and had less dense forest

[1]Institute of Environmental Science and Geography, University of Potsdam, Potsdam, Germany. [2]Institute of Geosciences, University of Potsdam, Potsdam, Germany. *e-mail: oliver.korup@geo.uni-potsdam.de

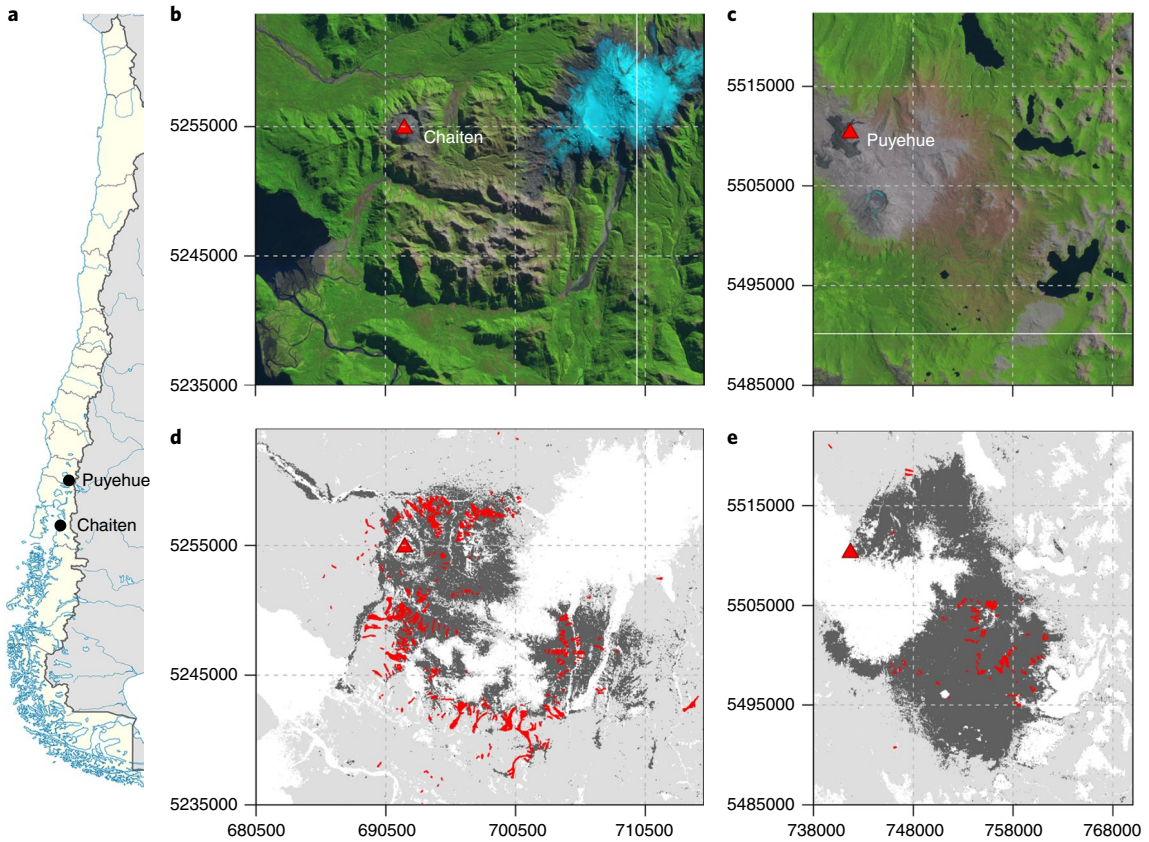

Fig. 1 | Satellite images of the Chaitén and Puyehue volcanoes, along with post-eruptive forest losses. a, Location of the Chilean volcanoes studied. **b**, Sentinel-2A satellite image of Chaitén Volcano (red triangle), south-central Chile (scene number T18GXT/T18GYT A009488; 16 April 2017). The thick white line is the boundary between scenes. **c**, Sentinel-2A satellite image of the Puyehue–Cordón Caulle volcanic complex. The red triangle shows the vent of the 2011 eruption (scene number T18GYA/T19GBQ A008344; 26 January 2017). **d**,**e**, Forests with >90% tree cover in 2000 (light grey), forest losses between 2000 and 2014 (dark grey[18]) and post-eruptive landslides (red) for Chaitén (**d**) and the Puyehue–Cordón Caulle volcanic complex (**e**). White areas include bare rock surfaces, water, ice, grass and shrub cover. The projection is UTM18S. Dashed lines mark coordinate grid. Credits: **a**, US Geological Survey; **b**,**c**, European Space Agency; **d**,**e**, Hansen/UMD/Google/USGS/NASA.

cover before the eruption. Almost all post-eruptive slope failures occurred in formerly dense forests with a nominal tree cover of >90%. Dozens of landslides cluster on Chaitén Volcano's northern slope and to the southeast of it where tephra cover was thickest, whereas at Puyehue most landslides affected leeward slopes east of the volcano. The time stamps of the satellite images offer approximate ages of forest disturbance and landslide occurrence[18]. We find that 80% of the landslides (and >90% of their total area) around Chaitén occurred in rainforests that the eruption had killed more than two (and mostly four) years before. Post-eruptive landslides in damaged forests around Puyehue had shorter delays and were fewer, as the eruption was more recent and the proportion of area above the treeline higher (Fig. 4). Nearly 90% of all post-eruptive slope failures happened some four years after trees were killed, mostly in areas where tephra was 0.1–0.5 m thick. Field checks of landslide scars and deposits confirmed mostly shallow (<2 m) failures that detached from the contact between soil and granitic and granodioritic bedrock within stands of mature dead trees in growth position. These landslides stripped mostly soil and vegetation, and minor amounts of debris, from bedrock slopes (Fig. 5). We estimate that these landslides mobilized $14.7^{+3.0}_{-3.0} \times 10^6\,m^3$ and $3.3^{+0.7}_{-0.7} \times 10^6\,m^3$ of soil and debris (excluding any pyroclastic fallout) around Chaitén and Puyehue, respectively, lowering the landscape within 30 km of each volcano by 1.1–4.8 mm on average (see Methods, Table 1 and Fig. 6). Assuming an original above-ground biomass of 110–510 t C ha^{-1} for the disturbed tree stands—based on a range of estimates reported for Chilean temperate rainforests on hillslopes[19] (Supplementary Table 5)—we infer that post-eruptive landslides pushed some 0.15–0.68 MtC of dead biomass into or near the drainage network. Eroded forest soils have been deposited on

Table 1 | Estimated cumulative area, volume and resulting average landscape lowering by post-eruptive landslides within various distances from the Puyehue and Chaitén volcanoes

	Distance from volcano (km)		
	10	20	30
Puyehue (<5 years)			
Landslide area (km^2)	0.1	1.9	2.5
Landslide volume (10^6 m^3)	$1.3^{+0.3}_{-0.3}$	$2.6^{+0.5}_{-0.5}$	$3.3^{+0.6}_{-0.6}$
Mean denudation (mm)	$0.4^{+0.08}_{-0.08}$	$2.1^{+0.4}_{-0.4}$	$1.1^{+0.2}_{-0.2}$
Chaitén (<8 years)			
Landslide area (km^2)	4.9	9.3	10.8
Landslide volume (10^6 m^3)	$6.3^{+1.2}_{-1.2}$	$12.4^{+2.5}_{-2.5}$	$13.6^{+2.8}_{-2.8}$
Mean denudation (mm)	$20.0^{+3.9}_{-3.9}$	$9.9^{+2.0}_{-2.0}$	$4.8^{+1.0}_{-1.0}$

Errors refer to ±1 s.d. about the posterior predictive mean (Fig. 6b).

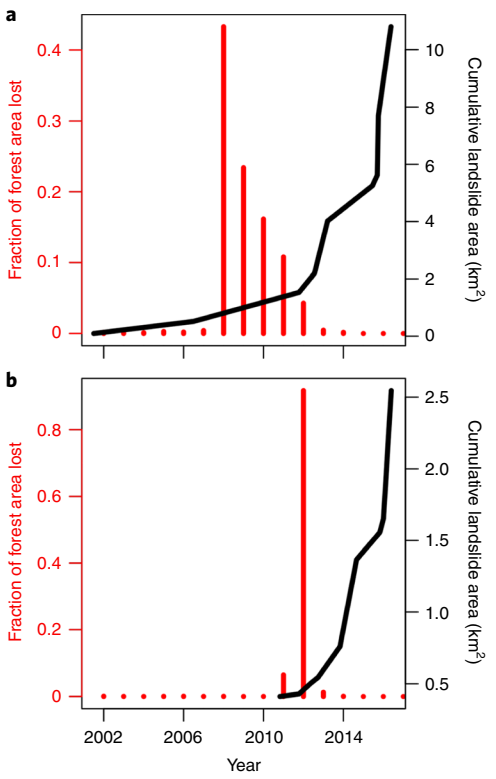

Fig. 2 | Time series of forest loss and landslide disturbance following the recent eruptions of the Chaitén and Puyehue volcanoes. a,**b**, Forest loss[18] and landslide disturbance are shown in red and black, respectively, for Chaitén (**a**) and Puyehue (**b**). The area of forest loss is normalized by the total forest area lost around each volcano between 2000 and 2014 (Fig. 1).

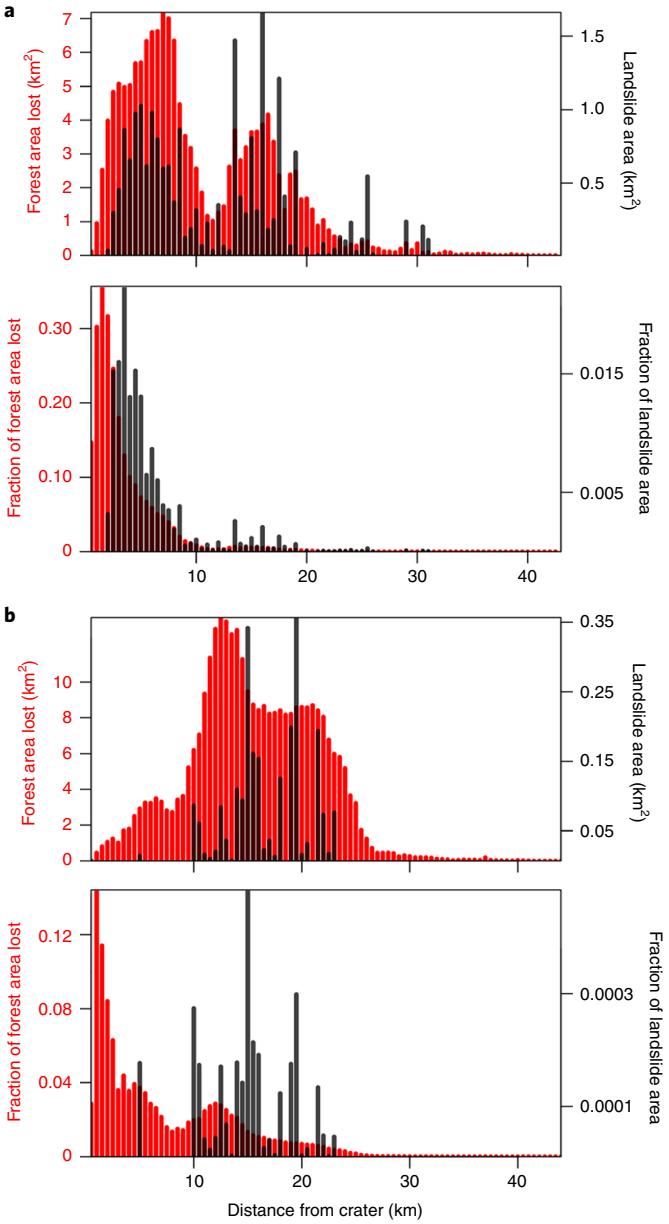

Fig. 3 | Histograms of absolute and relative areas of post-eruptive forest losses and landslide disturbance with increasing distance from the craters of the Chaitén and Puyehue volcanoes. a,**b**, Total (top) and fractional (bottom) post-eruptive forest losses (red) and landslide disturbances (dark grey) for Chaitén (**a**) and Puyehue (**b**). Relative areas are expressed as fractions of the circular areas for a given radial distance from the craters.

floodplains and coastal river deltas below Chaitén Volcano[8], but the fraction of landslide-borne material in this intermittent storage remains unknown. Reworked soil in landslide debris has an organic carbon content of $4.6^{+6.4}_{-3.0}$%, which is less than the ~7% in undisturbed floodplain soils nearby[8]. Assuming bulk densities of 0.8–1.1 t m^{-3} of landslide deposits, we estimate that, in total, shallow landslides eroded between $0.67^{+0.14}_{-0.14}$ and $0.92^{+0.19}_{-0.19}$ MtC of forest soils adjacent to the two volcanoes.

The satellite-derived survey of forest loss was originally intended to quantify regional changes[18], but it highlights how most landslides detached in forests classified as 'lost' after Chaitén and Puyehue erupted. Field surveys showed that forest disturbance ranged from complete tree removal due to lateral blasts near Chaitén's crater to abraded foliage and the snapping of branches due to tephra fall[20]. We find that landslides to the northeast of Chaitén's crater occurred in defoliated tree stands; landslides >10 km from the crater mostly initiated in forest stands with mature defoliated trunks in growth position. Most landslides around the volcano happened where tephra had covered forests by >0.1 m—a thickness that can seriously damage large trees[21]. Plot studies in stands of mostly *Nothofagus pumilio* around Puyehue Volcano showed a tree mortality of >50% where the tephra was 0.5 m thick[22]. Nearly 80% of all landslides happened at least two years after the eruptions, eroding gaps into damaged forests fringing the volcanoes; hence, we can exclude that slope failure caused the forest dieback. Instead, our time series show that forest dieback preceded, and probably caused, the landslides, given the close spatial matching. Compared with the post-eruptive landslides at Chaitén, fewer landslides emerged after the younger eruption at Puyehue, but with a similar delay and clustering downwind of the volcano. We infer that the disturbed forests primed slopes for instability in response to the eruptions via several possible mechanisms.

Links between forest dieback and slope instability

Thick tephra loads toppled numerous trees and uprooted soils[14,20], thus destabilizing hillslopes. Gradual loss of leaves, twigs and branches during dieback will lower rainfall interception and thus alter infiltration or runoff rates, and changing root-water uptake may add to a lagged landslide response. Moreover, tephra layers >5 cm thick can impede gas exchange between the atmosphere and the rhizosphere, reducing oxygen saturation and redox potential, probably provoking plant-root stress[23,24]. The Chaitén tephra fallout potentially increased toxic boron, cadmium, zinc, titanium,

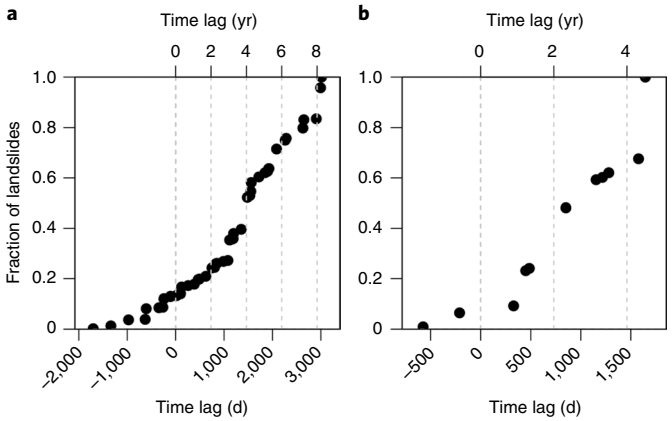

Fig. 4 | Cumulative distributions of estimated time lags between landslide occurrence and forest loss following the eruptions of the Chaitén and Puyehue volcanoes. a,**b**, Distributions of time lags for landslides with known maximum age at Chaitén (**a**; $n=540$) and Puyehue (**b**; $n=108$). We approximated the earliest date of each landslide for each volcano from the most recent time stamps of satellite images showing undisturbed conditions, with a uniform error of <183 d. The timing of forest loss[18] is documented to the nearest year. Negative time lags mark landslides that initiated forest disturbance mostly before the eruptions.

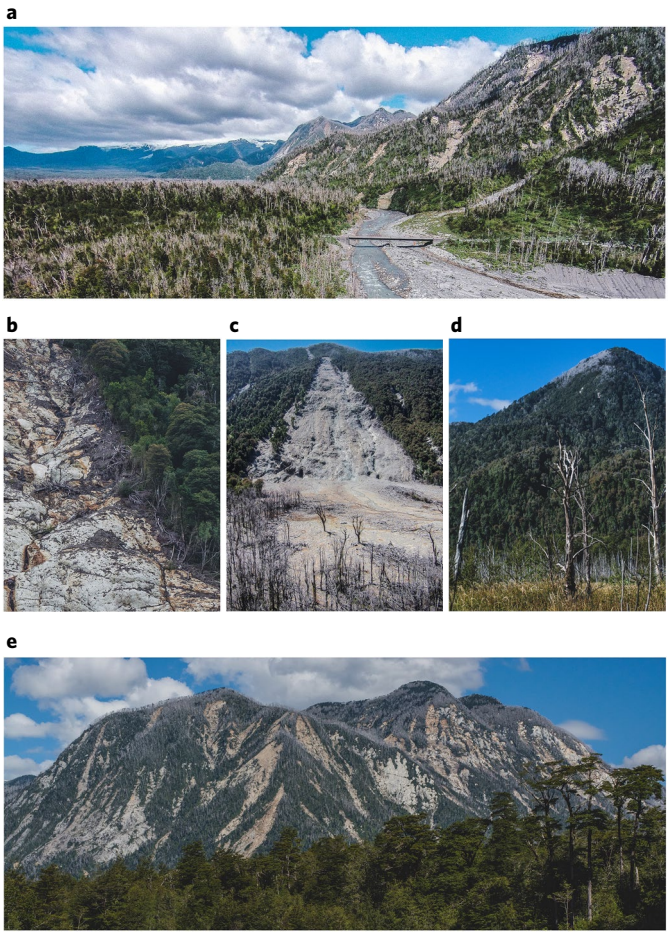

Fig. 5 | Post-eruptive landslides in disturbed temperate rainforests around Chaitén Volcano. Pale and defoliated tree trunks show dieback caused by the 2008 eruption. **a**, Upstream view of Rayas River undercutting landslide-dotted northeastern slopes of the volcano. **b**, Bedrock exposed in a landslide scar (Supplementary Fig. 5). **c**, A large landslide at Blanco River deposited some 0.2×10^6 m^3 of soil and debris on the floodplain. The scar is 360 m wide at the base. **d**, Patch of pale trees killed by tephra loads on a hilltop (background) 20 km southeast of the volcano. **e**, Shallow landslides clustered in dead forest patches about 5 km northeast of the crater.

copper, nickel and cobalt concentrations in living vegetation where the tephra fall was >2 mm thick[25]. Toxic fallout may acidify soils[26] and mobilize toxic levels of aluminium, leaching soil exchangeable cations that plants depend on. The accumulated effects of soil acidification, reduced soil aeration and lowered photosynthesis due to stomata plugged by ash[27] probably contributed to the widespread tree mortality. Other controls include forest species composition[20,22], closeness to the eruption source and topographic effects on wind fields and tephra thickness, possibly explaining why many of the landslides originated along upper ridge crests. Several episodes of massive flowering and dieback of *Chusquea* bamboo affected forests near Puyehue in 2011 and 2015. This may have also altered the protective vegetation cover[28] and thus, potentially, slope stability. These episodes may have caused minor fractions of forest loss, but do not fully explain the clustering of post-eruptive landslides downwind of the vent where tephra fall was thickest[15].

Regional and longer-term relevance

Regardless of the mechanisms at play, the biogeomorphic impacts of post-eruptive landslides are substantial. Lahars south of Chaitén Volcano reworked at least 11×10^6 m^3 of mostly pyroclastic sediment, and about $2.5–4.5\times10^6$ m^3 entered the fan delta of the Blanco River in the four years following the eruption of Chaitén Volcano[2,29]. Our results indicate that landslides later on recruited at least as much volume of hillslope materials from disturbed forest patches over a similar period. The forest biomass was eroded at an average of 265 ± 19 tC km^{-2} yr^{-1} in the first 8 years following the 2008 eruption. This organic carbon yield is among the highest reported worldwide[30,31]. More than 2.6×10^6 m^3 of fresh pyroclastic sediment prograded into Lake Puyehue south of the volcano in the two years after the eruption[15]. There, we estimate that post-eruptive landslides detached about the same volume of soil and debris in subsequent years. This overall post-eruptive denudation involved mainly soil and biomass, whereas rock-slope failure and hence bedrock erosion were negligible. Between 2012 and 2015, post-eruptive landslides around Chaitén moved at least three times the organic carbon that the surrounding rivers eroded from volcanically disturbed floodplains (~0.21 MtC)[8]. From a regional and longer-term perspective, explosive eruptions may be previously overlooked generators of sediment and terrestrial organic carbon pulses into the Patagonian fjords, probably contributing to the rapid burial rates in those important sinks[32]. We estimate that at least 0.44 GtC of forest biomass is within 30 km of 56 volcanoes in the SVZ (Supplementary Fig. 6). Assuming conservative estimates of forest biomass and soil organic carbon, together with published recurrence intervals of explosive eruptions of a magnitude comparable to the recent ones at Puyehue and Chaitén, we estimate that post-eruptive landslides may mobilize between 0.4 and 10 tC km^{-2} yr^{-1} on average from disturbed forests within 30 km of a given volcano (Supplementary Table 6). Yet, such millennial projections unduly smother the distinctly delayed and highly pulsed sediment and biomass fluxes that characterize this protracted volcanic hazard.

To conclude, following two recent eruptions in the SVZ, a sudden rise in landslide activity was concentrated on hillslopes that were densely forested before the eruptions but suffered thick tephra fall that killed or substantially damaged mature rainforest stands shortly after. Slope instability increased gradually in forest areas most affected by these eruptions; thus, the increase in landslides was not triggered during a single rainstorm. Instead, time series of slope instability are consistent with a lagged response to diminishing

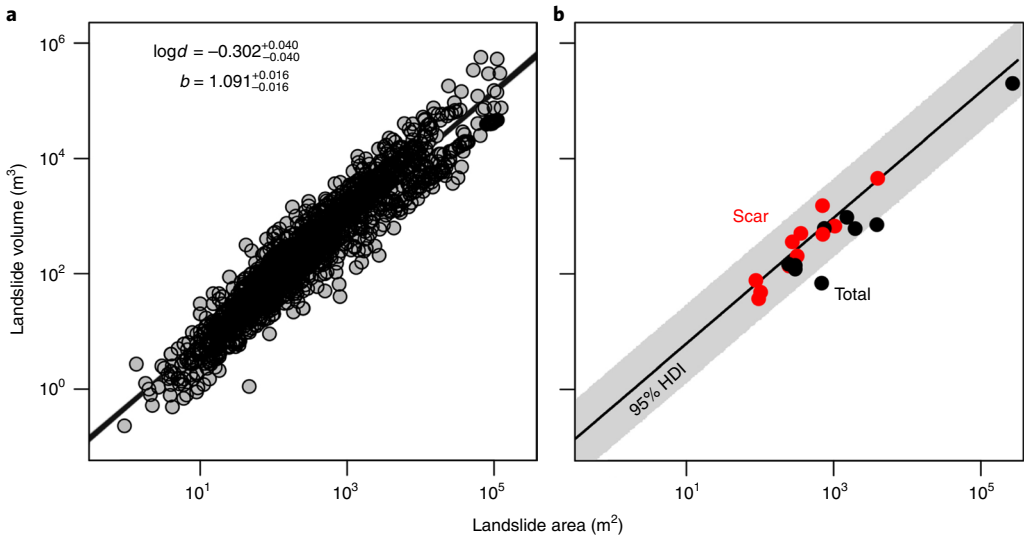

Fig. 6 | Prediction of landslide volume from footprint area. a, Empirical scaling between field-measured volume V (m^3) and footprint area A (m^2) of $n = 2{,}007$ soil landslides worldwide, assuming $V = dA^b$, where parameters d and b depend on material type (ref. [36]). The black line is the credible fit from Bayesian robust linear regression. **b**, Posterior predictive mean (black line) with 95% HDI (grey). Points are $n = 20$ post-eruptive landslides around Chaitén Volcano, derived from high-resolution digital topography obtained by drone surveys (this study). 'Landslide area' refers to either scar or total affected area; the prediction is based on a mix of both types of data, and encompasses mean landslide depths of 0.8–1.8 m.

tree-root strength and slowly regrowing vegetation, offering a time window for widespread landsliding mostly four to eight years after volcanic disturbance. Such a delayed response agrees well with observations from logging and deforestation, where decaying tree roots and uprooted trees promote landslides several years after the disturbance[33–35]. We quantified post-eruptive slope failure as a delayed and pulsed volcanic hazard in forested hillslopes disturbed by tephra. Our results emphasize the need to consider biogeomorphic controls on erosion, transport and deposition on hillslopes and in river channels in response to volcanic disturbances. Monitoring and quantifying such a response may need to continue well beyond a few years to also capture the delayed flushing of soils and biomass from forested hillslopes, so that we can better gauge the associated hazards and risks to buildings, infrastructure and land-use resources.

Online content

Any methods, additional references, Nature Research reporting summaries, source data, statements of data availability and associated accession codes are available at https://doi.org/10.1038/s41561-019-0315-9.

Received: 9 March 2018; Accepted: 29 January 2019;
Published online: 4 March 2019

References

1. Major, J. J. & Yamakoshi, T. Decadal-scale change of infiltration characteristics of a tephra-mantled hillslope at Mount St Helens, Washington. *Hydrol. Proc.* **19**, 3621–3630 (2005).
2. Pierson, T. C., Major, J. J., Amigo, Á. & Moreno, H. Acute sedimentation response to rainfall following the explosive phase of the 2008–2009 eruption of Chaitén volcano, Chile. *Bull. Volcanol.* **75**, 723 (2013).
3. Korup, O. Earth's portfolio of extreme sediment transport events. *Earth Sci. Rev.* **112**, 115–125 (2012).
4. National Academies of Sciences, Engineering and Medicine *Volcanic Eruptions and Their Repose, Unrest, Precursors, and Timing* (National Academies Press, 2017).
5. Veblen, T. T. & Ashton, D. H. Catastrophic influences on the vegetation in the Valdivian Andes, Chile. *Vegetatio* **36**, 149–167 (1978).
6. Grubb, P. J., Bellingham, P. J., Kohyama, T. S., Piper, F. I. & Valido, A. Disturbance regimes, gap-demanding trees and seed mass related to tree height in warm temperate rain forests worldwide. *Biol. Rev.* **88**, 701–744 (2013).
7. Capra, L. et al. Rainfall-triggered lahars at Volcan de Colima, Mexico: surface hydro-repellency as initiation process. *Bull. Volcan. Geotherm. Res.* **189**, 105–117 (2010).
8. Mohr, C. H., Korup, O., Ulloa, H. & Iroumé, A. Pyroclastic eruption boosts organic carbon fluxes into Patagonian fjords. *Glob. Biogeochem. Cycles* **31**, 1626–1638 (2017).
9. Keim, R. F. & Skaugset, A. E. Modelling effects of forest canopies on slope stability. *Hydrol. Proc.* **17**, 1457–1467 (2003).
10. Imaizumi, F., Sidle, R. C. & Kamei, R. Effects of forest harvesting on the occurrence of landslides and debris flows in steep terrain of central Japan. *Earth Surf. Proc. Landf.* **33**, 827–840 (2008).
11. Walsh, R. P. D. et al. Long-term responses of rainforest erosional systems at different spatial scales to selective logging and climate change. *Phil. Trans. R. Soc. Lond. B* **366**, 3340–3353 (2011).
12. Singer, B. S. et al. Eruptive history, geochronology, and magmatic evolution of the Puyehue–Cordón Caulle volcanic complex, Chile. *Geol. Soc. Am. Bull.* **120**, 599–618 (2008).
13. Carn, S. et al. The unexpected awakening of Chaitén volcano, Chile. *EOS Trans.* **90**, 205–212 (2009).
14. Alfano, F. et al. Tephra stratigraphy and eruptive volume of the May, 2008, Chaitén eruption, Chile. *Bull. Volcanol.* **73**, 613–630 (2011).
15. Bertrand, S., Daga, R., Bedert, R. & Fontijn, K. Deposition of the 2011–2012 Cordón Caulle tephra (Chile, 40°S) in lake sediments: implications for tephrochronology and volcanology. *J. Geophys. Res. Earth Surf.* **119**, 2555–2573 (2014).
16. Myers, N., Mittermeier, R. A., Mittermeier, C. G., da Fonseca, G. A. B. & Kent, J. Biodiversity hotspots for conservation priorities. *Nature* **403**, 853–858 (2000).
17. Pollmann, W. & Veblen, T. T. Nothofagus regeneration dynamics in south-central Chile: a test of a general model. *Ecol. Monogr.* **74**, 615–634 (2004).
18. Hansen, M. C. et al. High-resolution global maps of 21st-century forest cover change. *Science* **342**, 850–853 (2013).
19. Urrutia-Jalabert, R., Malhi, Y. & Lara, A. The oldest, slowest rainforests in the world? Massive biomass and slow carbon dynamics of *Fitzroya cupressoides* temperate forests in southern Chile. *PLoS ONE* **10**, e0137569 (2015).
20. Swanson, F. J., Jones, J. A., Crisafulli, C. M. & Lara, A. Effects of volcanic and hydrologic processes on forest vegetation: Chaitén Volcano, Chile. *Andean Geol.* **40**, 359–391 (2013).
21. Arnalds, O. The influence of volcanic tephra (ash) on ecosystems. *Adv. Agron.* **121**, 331–380 (2013).
22. Swanson, F. J., Jones, J., Crisafulli, C., González, M. E. & Lara, A. Puyehue–Cordón Caulle eruption of 2011: tephra fall and initial forest responses in the Chilean Andes. *Bosque* **37**, 85–96 (2016).
23. Ayris, P. M., & Delmelle, P. The immediate environmental effects of tephra emission. *Bull. Volcanol.* **74**, 1905–1936 (2012).

24. Hotes, S., Poschlod, P., Takahashi, H., Grootjans, A. P. & Adema, E. Effects of tephra deposition on mire vegetation: a field experiment in Hokkaido, Japan. *J. Ecol.* **92**, 624–634 (2004).
25. Martin, R. S. et al. Environmental effects of ashfall in Argentina from the 2008 Chaitén volcanic eruption. *J. Volcan. Geotherm. Res.* **184**, 462–472 (2009).
26. Blackford, J. J., Edwards, K. J., Dugmore, A. J., Cook, G. T. & Buckland, P. C. Icelandic volcanic ash and the mid-Holocene Scots pine (*Pinus sylvestris*) pollen decline in northern Scotland. *Holocene* **2**, 260–265 (1992).
27. Hinckley, T. M. et al. Impact of tephra deposition on growth in conifers: the year of the eruption. *Can. J. Forest Res.* **14**, 731–739 (1984).
28. De la Fuente, A & Pacheco, N. Biomass, seed production and phenology of *Chusquea montana* after a massive and synchronous flowering event in Puyehue National Park, Chile. *Bosque* **38**, 601–606 (2017).
29. Major, J. J. et al. Extraordinary sediment delivery and rapid geomorphic response following the 2008–2009 eruption of Chaitén Volcano, Chile. *Water Resour. Res.* **52**, 5075–5094 (2016).
30. Hilton, R. G., Galy, A. & Hovius, N. Riverine particulate organic carbon from an active mountain belt: importance of landslides. *Glob. Biogeochem. Cycles* **22**, GB1017 (2008).
31. Clark, K. E. et al. Storm-triggered landslides in the Peruvian Andes and implications for topography, carbon cycles, and biodiversity. *Earth Surf. Dynam.* **4**, 47–70 (2016).
32. Smith, R. W., Bianchi, T. S., Allison, M., Savage, C. & Galy, V. High rates of organic carbon burial in fjord sediments globally. *Nat. Geosci.* **8**, 450–453 (2015).
33. Sidle, R. C. A conceptual model of changes in root cohesion in response to vegetation management. *J. Environ. Qual.* **20**, 43–52 (1991).
34. Schmidt, K. M. et al. The variability of root cohesion as an influence of shallow landslide susceptibility in the Oregon Coast Range. *Can. Geotech. J.* **38**, 995–1024 (2001).
35. Pierson, T. C. & Major, J. J. Hydrogeomorphic effects of explosive volcanic eruptions on drainage basins. *Ann. Rev. Earth Planet. Sci.* **42**, 469–507 (2014).

Acknowledgements

This work was partly funded by the projects CONICYT-BMBF PCCI20130045 and BMBF 01DN13060, courtesy of the German Federal Ministry of Education and Research. We thank A. Iroumé and E. Parra for help with logistics, and appreciate the support of E. Gonzalez and the rangers at Pumalín National Park, as well as the Dirección General Aeronautica Civil for permitting UAV flights. We thank J. J. Major for comments on the manuscript. We ran all computations using the statistical environment R (www.r-project.org).

Author contributions

O.K. and C.H.M. collected the field data. O.K. and J.S. analysed the data. O.K. designed the study and wrote the manuscript, with input from J.S. and C.H.M.

Competing interests

The authors declare no competing interests.

Additional information

Supplementary information is available for this paper at https://doi.org/10.1038/s41561-019-0315-9.

Reprints and permissions information is available at www.nature.com/reprints.

Correspondence and requests for materials should be addressed to O.K.

Publisher's note: Springer Nature remains neutral with regard to jurisdictional claims in published maps and institutional affiliations.

© The Author(s), under exclusive licence to Springer Nature Limited 2019

Methods

We used remote-sensing images (Landsat satellites 7 and 8 and Sentinel-2A at 30 and 10 m resolution, respectively) to map the outline of landslide scars, runout tracks and deposits within an arbitrary radius of 40 km around the Chaitén and Puyehue volcanoes, given that volcanic fallout was mostly >0.01 m in that perimeter[14]. We identified landslides as elongate, hairpin-shaped and highly reflective patches in the dense evergreen forest cover prevalent in our study area. Our landslide maps approximately capture areas disturbed by slope instability, given the possibility of: (1) confusing landslides with bedrock bluffs, cascades and snow-avalanche tracks; (2) overlooking landslides in the shadows of steep valleys; and (3) coalesced runout tracks and deposits. For several freshly formed debris-flow fans we could not discern with certainty their sources of sediment. We estimated the earliest date of each landslide from the time stamp of the image immediately predating the one on which the landslide appeared first. Landslide scars remained clearly visible for at least a decade after their first appearance, so that we assume that our oldest mapped landslides occurred in the late 1990s at least. The NDVI records, in detail, the browning and re-greening of forests covered by the thickest air-fall deposits that we estimated from field reports[14]. We used a global forest change inventory of estimated forest losses, defined as 'stand-replacement disturbance or the complete removal of tree cover canopy', and derived from NDVI data in Landsat time series between 2000 and 2014 at a nominal resolution of 30 m[18]. We checked 21 landslides in the field and estimated their average thickness in lower scar areas based on orthophotos draped on 0.25 m digital elevation models that we generated with structure-from-motion mapping using a DJI Mavic Pro and eBee RTK unmanned aerial vehicle (UAV). We used Bayesian robust linear regression to predict the landslide volume, V (m^3), from its footprint area, A (m^2), using the scaling relationship $V = dA^b$, where parameters d and b depend on material type, and field data on $n = 2{,}007$ soil landslides[36]. For a mixed sample of scar and total affected areas of these landslides, we obtained posterior mean estimates of $\log[d] = -0.302^{+0.040}_{-0.040}$ and $b = 1.091^{+0.016}_{-0.016}$ (errors enclose the 95% highest density interval (HDI); Fig. 6). We found that 90% of our UAV-derived landslide areas and volumes are within the 95% HDI of this prediction, so we adapted the scaling relationship for our landslide inventory. Our volumetric estimate of the total landslide volume refers to the mean of the posterior predictive distributions plus or minus two standard deviations. To estimate the average mass of soil organic carbon removed by these landslides, we multiplied the landslide volume by the range of bulk soil density and the range of soil organic carbon content compiled from the literature (see Supplementary Information).

Data availability

The data that support the findings of this study are available from the corresponding author upon request. We used the publicly available Landsat and Sentinel-2 satellite imagery (https://earthexplorer.usgs.gov/ and https://sentinel.esa.int/) and Space Shuttle Radar Topgraphy Mission (https://earthexplorer.usgs.gov/) data to map the landslides. Our rainfall analysis draws on Chilean station data (http://www.cr2.cl/datos-de-precipitacion/). The Global Forest Inventory is available at http://earthenginepartners.appspot.com/science-2013-global-forest/download_v1.5.html.

References

36. Larsen, I. J., Montgomery, D. R. & Korup, O. Landslide erosion controlled by hillslope material. *Nat. Geosci.* **3**, 247–251 (2010).